0026-895X/95/061248-07$3.00/0

MOLECULAR PHARMACOLOGY, 47:1248–1254 (1995).

Cholinergic Inhibition of Slow Delayed-Rectifier K^+ Current in Guinea Pig Sino-atrial Node Is Not Mediated by Muscarinic Receptors

LISA C. FREEMAN[1] and ROBERT S. KASS

Department of Physiology, University of Rochester School of Medicine and Dentistry, Rochester, New York 14642-8642

Received December 14, 1994; Accepted March 10, 1995

SUMMARY

We studied the effects of cholinergic agonists on slow delayed-rectifier K^+ current (I_{Ks}) in isolated cells from the sino-atrial node (SAN) region of guinea pig heart, using patch-clamp procedures. Carbachol (5 nM to 10 μM) inhibited I_{Ks} in guinea pig SAN cells in the absence of previous β-adrenergic stimulation and in cells pretreated with 8-(4-chlorophenylthio)-cAMP. Neither the muscarinic antagonist atropine nor the nicotinic antagonist hexamethonium antagonized carbachol inhibition of the current. Similar results were obtained with other cholinergic agonists. Cholinergic stimulation of the muscarinic K^+ current was successfully antagonized by atropine in SAN cells where inhibition of I_{Ks} persisted. Therefore, the lack of antagonist effects on inhibition of I_{Ks} cannot be attributed to either an absence of muscarinic cholinoceptors on SAN cells or a loss of antagonist activity under our experimental conditions. These data demonstrate that cholinergic agonists, including the endogenous neurotransmitter acetylcholine, decrease the amplitude of I_{Ks} in guinea pig SAN cells via a non-muscarinic, non-nicotinic, cAMP-independent mechanism. Although the precise nature of this signal transduction pathway has not been elucidated, it is clearly different from those described for regulation of other nodal currents. Differential regulation of I_{Ks} in guinea pig SAN and ventricle cannot be attributed to higher basal adenylate cyclase activity in SAN cells. The inhibitory effect of carbachol on I_{Ks} was not additive with that of verapamil, a drug that is both an allosteric muscarinic antagonist and a potassium channel-blocking agent. Cholinergic agonists may inhibit I_{Ks} in SAN cells via a direct interaction with the SAN I_{Ks} channel.

Cholinergic regulation of ionic currents has been demonstrated in ventricular, atrial, and SAN cells isolated from amphibian and mammalian hearts. Regulation of ionic currents in SAN has been extensively investigated, because muscarinic control of heart rate is physiologically important. It has been shown that inhibition of I_{Ca} and I_f by muscarinic agonists occurs via a different mechanism in SAN cells, compared with ventricular myocardium (1).

Muscarinic agonists can inhibit I_f in Purkinje fibers (2), as well as I_{Ca} and I_{Ks} in ventricular myocytes, in the presence but not the absence of previous β-adrenergic stimulation (1–5). In contrast, in isolated cells from mammalian SAN, muscarinic agonists inhibit these ionic currents in the absence of previous β-adrenergic stimulation (1, 5–7). The primary signal transduction pathway underlying muscarinic inhibition of I_f and I_{Ca} in rabbit SAN cells involves a reduction in cAMP levels mediated by receptors of the M2 subtype and pertussis toxin-sensitive G proteins (1, 5, 7), although membrane-delimited, G protein-dependent regulation of I_f by muscarinic receptors has also been described (8). On this basis, it has been hypothesized that SAN cells have higher basal adenylate cyclase activity and, consequently, higher basal concentrations of cAMP than do ventricular myocytes (1, 5, 7). Because both I_{Ca} and I_f are believed to contribute to the pacemaker potential (9), it has been further speculated that high basal adenylate cyclase activity is a distinctive property of SAN cells that allows fine modulation of ionic currents that underlie pacemaker activity (1, 5).

Although regulation of the SAN I_K has also been implicated in the control of heart rate (9, 10), modulation of I_K by adrenergic and cholinerigc agonists has not been extensively investigated in isolated SAN cells. Patch-clamp experiments designed to characterize neurotransmitter effects on I_K in mammalian heart have been performed primarily using

This work was supported by United States Public Health Service Grant HL44365.

[1] Present address: Department of Anatomy and Physiology, College of Veterinary Medicine, Kansas State University, Manhattan, KS 66506-5602.

ABBREVIATIONS: SAN, sino-atrial node; I_{Ks}, slow delayed-rectifier K^+ current; I_{Ca}, L-type Ca^{2+} current; I_f, hyperpolarization-activated inward K^+ current; I_K, delayed-rectifier K^+ current; I_{Kr}, rapidly activating, rectifying K^+ current; 8-CPT-cAMP, 8-(4-chlorophenylthio)-cAMP; *Sp*-5,6-DCl-cBIMPS, *Sp*-5,6-dichlorobenzimidazole-1-β-D-ribofuranoside 3′,5′-cyclic phosphorothioate; minK, minimal K^+; $I_{K\text{-}ACh}$, muscarinic K^+ current; HEPES, 4-(2-hydroxyethyl)-1-piperazineethanesulfonic acid; EGTA, ethylene glycol bis(β-aminoethyl ether)-*N*,*N*,*N*′,*N*′-tetraacetic acid; ACh, acetylcholine.

guinea pig myocytes (3, 4, 11), whereas information about membrane currents in SAN cells has been obtained primarily from whole-cell patch-clamp experiments on cells isolated from rabbit SAN (9, 12). It is difficult to make general statements about nodal I_K based on the available data, because repolarizing K^+ currents in these two preparations are not similar. In guinea pig heart, I_K consists of two components, I_{Kr} and the noninactivating I_{Ks} (13); however, in rabbit heart only I_{Kr} is present (14). I_{Ks} but not I_{Kr} can be enhanced by β-adrenergic stimulation (15). I_{Ks} is also enhanced by other treatments that increase intracellular cAMP levels (3, 4, 6, 11).

Like I_f and I_{Ca} in rabbit SAN, I_{Ks} in cells from the SAN region of guinea pig heart is inhibited by the muscarinic agonist carbachol in the absence of previous β-adrenergic stimulation (6). However, the signal transduction pathways that underlie inhibition of guinea pig SAN I_{Ks} have not been described. Here, we present data that suggest that the mechanism responsible for cholinergic inhibition of I_{Ks} in guinea pig SAN is distinct from those described previously for muscarinic inhibition of other nodal ionic currents. A preliminary report of these results has appeared (16).

Materials and Methods

Cell isolation. Methods for isolating cells from the SAN region of adult guinea pig heart have been described in detail elsewhere (17). Briefly, adult guinea pig hearts were retrogradely perfused with an enzyme-containing solution. SAN cells were isolated from the perinodal region, a 2-mm × 2-mm piece of tissue bordered by the crista terminalis and intra-atrial septum on two sides and by the cranial and caudal vena cava on the other two sides. Two additional criteria, morphology and electrophysiology, were then used for the identification of SAN cells. As described previously (17), SAN cells were spherical or spindle-shaped, with high input resistances (0.71–1 GΩ) and low total cell capacitance (~10 pF). In some instances, the presence of I_f and/or spontaneous oscillatory activity at 37° was also demonstrated.

Experimental solutions and data acquisition. Experimental results shown below were obtained using patch-clamp procedures in whole-cell (18) or perforated patch (19) configurations. Intra- and extracellular recording solutions designed to isolate K^+ currents have been described previously (6, 17). Patch pipettes (Clay Adams glass) were pulled to resistances of 2.5–5 MΩ when filled with intracellular solutions (110 mM potassium aspartate, 2 mM $MgCl_2$, 1 mM $CaCl_2$, 11 mM EGTA, 10 mM ATP, 10 mM HEPES, pH 7.3, which was adjusted with KOH to bring the final K^+ concentration to 140 mM). For perforated patch recording, nystatin was dissolved in methanol at a concentration of 50 mg/ml and then added to the standard internal solution to yield a final concentration of 100 μg/ml. Both the nystatin stock solution and the nystatin-containing pipette solution were subjected to 5–10 min of ultrasonication before use. External solutions consisted of 132 mM NaCl or sodium aspartate, 0–4.8 mM KCl, 1 mM $MgCl_2$, 5 mM glucose, 5 mM HEPES, and 1 mM $CaCl_2$, pH 7.4, adjusted with NaOH. I_{Ca} was blocked with nisoldipine (500 nM to 1 μM). I_{Kr} was blocked with E-4031 (5 μM).

The voltage-clamp protocol for current activation consisted of depolarizing pulses applied at a frequency of 0.2 Hz to various test potentials, for the durations indicated in each experiment. In all experiments, the holding potential was −40 mV. Current traces were low pass filtered at 2 kHz and sampled at 125 Hz. Data were stored and analyzed on an IBM-compatible 386 computer (Dell Computer Corp., Austin, TX) using pCLAMP software (Axon Instruments, Burlingame, CA). Experiments were carried out at either room temperature (20–22°) or 37°, as indicated. Unless otherwise stated, I_{Ks} was measured as the amplitude of tail current associated with a 3-sec depolarizing test pulse to +60 mV. Leak subtraction is noted where employed. For example, in Fig. 4, linear leak was estimated from $I_{K\text{-}ACh}$ records by extrapolation of a linear curve fitted to currents positive to 0 mV, and then leak currents were subtracted from total current measurements.

Drugs and chemicals. Carbachol (carbamylcholine chloride), atropine sulfate, methoctramine tetrahydrochloride, oxotremorine sesquifumarate, and OXA-22 (*cis*-2-methyl-5-trimethylammoniummethyl-1,3-oxathiolane iodide) were purchased from Research Biochemicals International (Natick, MA). 8-CPT-cAMP sodium salt was purchased from Boehringer Mannheim (Indianapolis, IN). *Sp*-5,6-DCl-cBIMPS was obtained from BioLog (La Jolla, CA). All other drugs and chemicals were purchased from Sigma Chemical Co. (St. Louis, MO).

Solutions were prepared freshly on each experimental day. Verapamil hydrochloride and 8-CPT-cAMP were dissolved in the external recording solution to yield 10× or 100× concentrated stock solutions. More concentrated (≥200×) stock solutions of the other drugs were prepared by dissolving the compunds in doubly distilled, deionized water.

Statistics. Data are expressed as mean ± standard error. Analysis of variance (repeated-measures design) was used to evaluate the statistical significance of various drug treatments. Differences were considered significant at $p < 0.05$. If a significant difference was found with the F test, individual means were compared using Tukey's procedure (Statistix; Analytical Software, Tallahassee, FL).

Results

I_{Ks} in cells isolated from the SAN region of guinea pig heart was recorded by applying a series of 3-sec depolarizing test pulses (−20 to +60 mV, step 20) from a holding potential of −40 mV. As expected (6), extracellular application of carbachol, a stable analogue of the endogenous neurotransmitter ACh, inhibited basal I_{Ks} in guinea pig SAN cells (Fig. 1). Fig. 1 shows the percentage of I_{Ks} remaining as a function of applied concentration for 1 nM ($n = 3$), 10 nM ($n = 3$), 100 nM ($n = 5$), 300 nM ($n = 7$), 500 nM ($n = 4$), 1 μM ($n = 4$), and 10 μM ($n = 2$) carbachol. Carbachol inhibition of I_{Ks} was evident at nanomolar concentrations, and the maximal effect of carbachol was obtained at 100 nM. Carbachol inhibited I_{Ks} at all test potentials, in a voltage-independent manner. Results identical to those shown in Fig. 1 were obtained when various concentrations of carbachol were applied to an individual cell.

Carbachol inhibition of I_{Ks} did not depend on intracellular dialysis with the pipette solution. Results obtained using the perforated patch technique were similar to those obtained using the whole-cell configuration of the patch-clamp technique. In three experiments that used the perforated patch technique, carbachol (500 nM) decreased I_{Ks} by 47 ± 7% ($n = 3$); the magnitude of I_{Ks} inhibition in these experiments was comparable to that shown in Fig. 1 (500 nM, 49 ± 6%, $n = 5$).

SAN region cells exhibit a relative variability in I_{Ks} amplitude (6, 17). To determine whether the inhibitory effect of carbachol on I_{Ks} could be correlated with current density, the effect of carbachol (1 μM) was examined in cells with different densities of I_{Ks} under control conditions. No significant relationship existed between the percentage of I_{Ks} inhibition by carbachol and the control current density ($n = 7$, correlation coefficient = 0.36).

To study the involvement of cAMP and protein kinase A in carbachol inhibition of I_{Ks}, we examined the effect of carbachol on I_{Ks} enhanced by the membrane-permeant cAMP an-

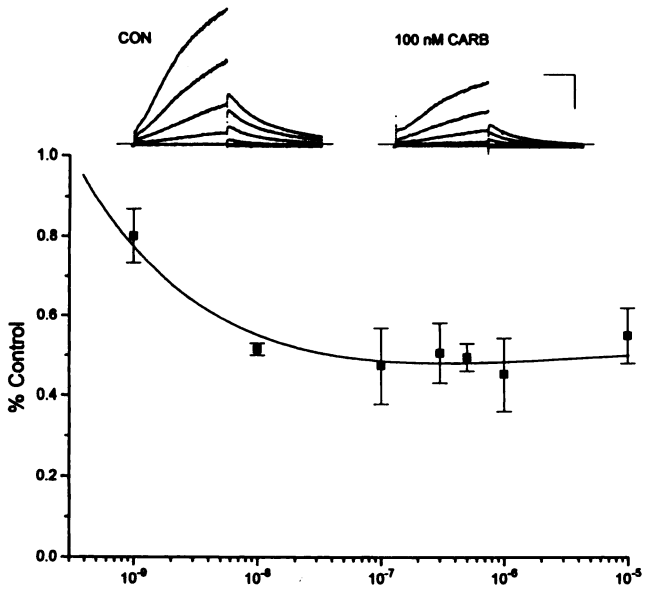

Fig. 1. Concentration-dependent inhibition of I_{Ks} induced by carbachol in isolated SAN cells from guinea pig heart. *Curve*, I_{Ks} measured as the amplitude of deactivating tail current after a 3-sec pulse to +60 mV at room temperature and expressed as a percentage of current measured under similar conditions in the absence of carbachol. Data are shown as mean ± standard error. The number of cells (*n*) studied for each concentration of carbachol is reported in the text. *Inset*, I_{Ks} elicited from an isolated SAN cell by a series of depolarizing test pulses (*bottom* to *top*, −20 to +60 mV, in steps of 20 mV) from a −40-mV holding potential, before (*CON*) and after (*CARB*) application of 100 nM carbachol. *Calibration bars*, 200 pA and 1 sec. Measurements were made in the whole-cell configuration, with an extracellular K^+ concentration of 0.5 mM, at 22°.

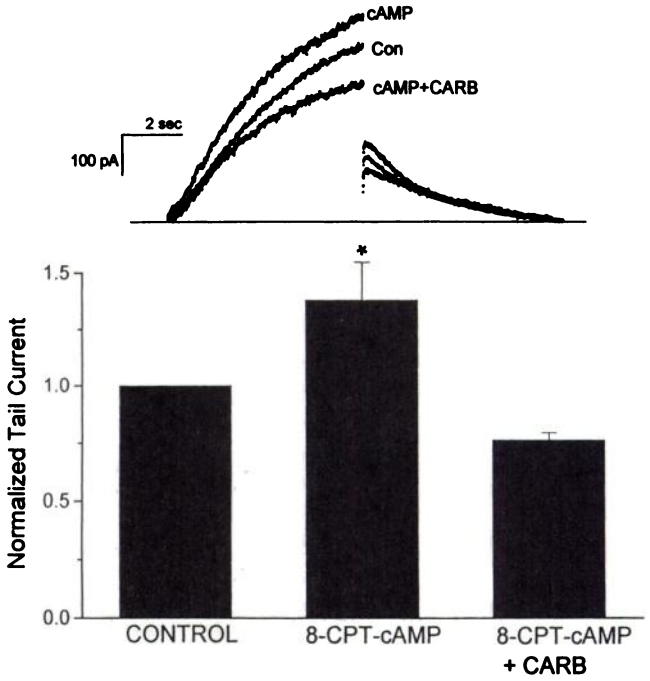

Fig. 2. Carbachol (*CARB*) inhibition of I_{Ks} stimulated with 8-CPT-cAMP. I_{Ks} recorded from guinea pig SAN cells was enhanced by extracellular application of 200 μM 8-CPT-cAMP, and cells were then exposed to 500 nM carbachol. *Upper*, I_{Ks} activated by a 3-sec depolarizing test pulse to +60 mV from a −40-mV holding potential, under control conditions (*Con*) and after subsequent exposure of the cell to 8-CPT-cAMP (*cAMP*) and then 8-CPT-cAMP plus CARB (*cAMP+CARB*). *Calibration bars*, 100 pA and 2 sec. Measurements were made in the whole-cell configuration, with an extracellular K^+ concentration of 0.5 mM, at 22°. Time-independent current, including linear leak, was subtracted. *Lower*, cumulative results from five experiments. I_{Ks} was measured as tail current amplitude after a 3-sec pulse to +60 mV, from a holding potential of −40 mV. *, Statistically significant difference in I_{Ks} amplitude.

alogue 8-CPT-cAMP (200 μM). As shown previously (6), extracellular application of 8-CPT-cAMP enhanced guinea pig SAN I_{Ks}. In these experiments, carbachol consistently inhibited I_{Ks}, which was enhanced by 8-CPT-cAMP (Fig. 2). Carbachol inhibition of the cAMP-enhanced current (500 nM, 42 ± 7%, n = 5) was not significantly different in magnitude from its inhibition of the basal current (500 nM, 49 ± 3%, n = 8). Similar results were obtained using another membrane-permeant cAMP analogue, *Sp*-5,6-DCl-cBIMPS (n = 2).

To determine whether carbachol inhibition of I_{Ks} was mediated by a muscarinic cholinoceptor, we examined the effect of the non-subtype-specific muscarinic antagonist atropine on basal I_{Ks} and on the carbachol-mediated reduction in current amplitude. Atropine had no significant effect on basal I_{Ks}. I_{Ks} amplitude was 146.1 ± 48.9 pA in the absence and 142.4 ± 54.5 pA in the presence of 500 nM atropine (n = 5). Atropine (0.3–1 μM) also failed to antagonize carbachol inhibition of I_{Ks}; pretreatment with atropine did not prevent carbachol inhibition of I_{Ks} (Fig. 3). Similar results were obtained with experiments using whole-cell or perforated patch configurations of patch clamp (Fig. 3, *upper* versus *lower*).

To determine whether the antagonist activity of atropine was compromised under our experimental conditions, we measured I_{Ks} and $I_{K\text{-}ACh}$ in the same SAN cells before and after application of carbachol and atropine, using the response of $I_{K\text{-}ACh}$ as a control. At concentrations of >1 μM in guinea pig SAN cells, carbachol not only inhibited I_{Ks} but also enhanced $I_{K\text{-}ACh}$; the effects of the endogenous muscarinic agonist ACh on I_{Ks} and $I_{K\text{-}ACh}$ were similar to those of carbachol (Fig. 4). In SAN cells, where atropine failed to

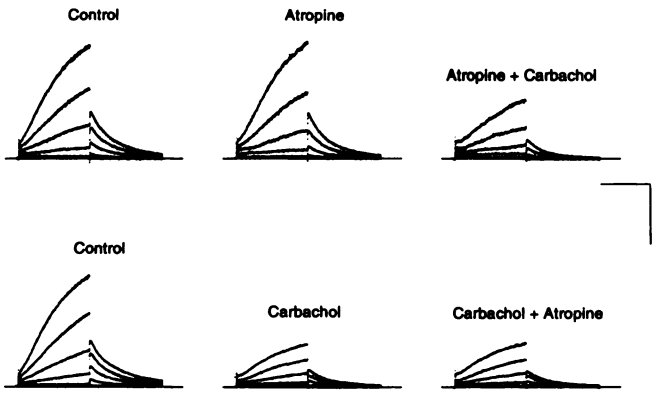

Fig. 3. Evidence that carbachol inhibition of I_{Ks} was not antagonized by the nonspecific muscarinic antagonist atropine. *Upper*, I_{Ks} elicited as described in Fig. 1, under control conditions and after extracellular application of 500 nM atropine and then 500 nM carbachol plus 500 nM atropine. Measurements were made in the whole-cell configuration, with an extracellular K^+ concentration of 0.5 mM, at 22°. *Calibration bars*, 250 pA and 2 sec. *Lower*, I_{Ks} elicited as described in Fig. 1, under control conditions and after extracellular application of 500 nM carbachol and then 500 nM carbachol plus 500 nM atropine. Measurements were made in the perforated patch configuration, with an extracellular K^+ concentration of 0.5 mM, at 22°. *Calibration bars*, 500 pA and 2 sec.

antagonize depression of I_{Ks} by carbachol or ACh, enhancement of $I_{K\text{-}ACh}$ was effectively reversed by atropine (Fig. 4). Effects of the subtype-specific M2 antagonist methoctramine

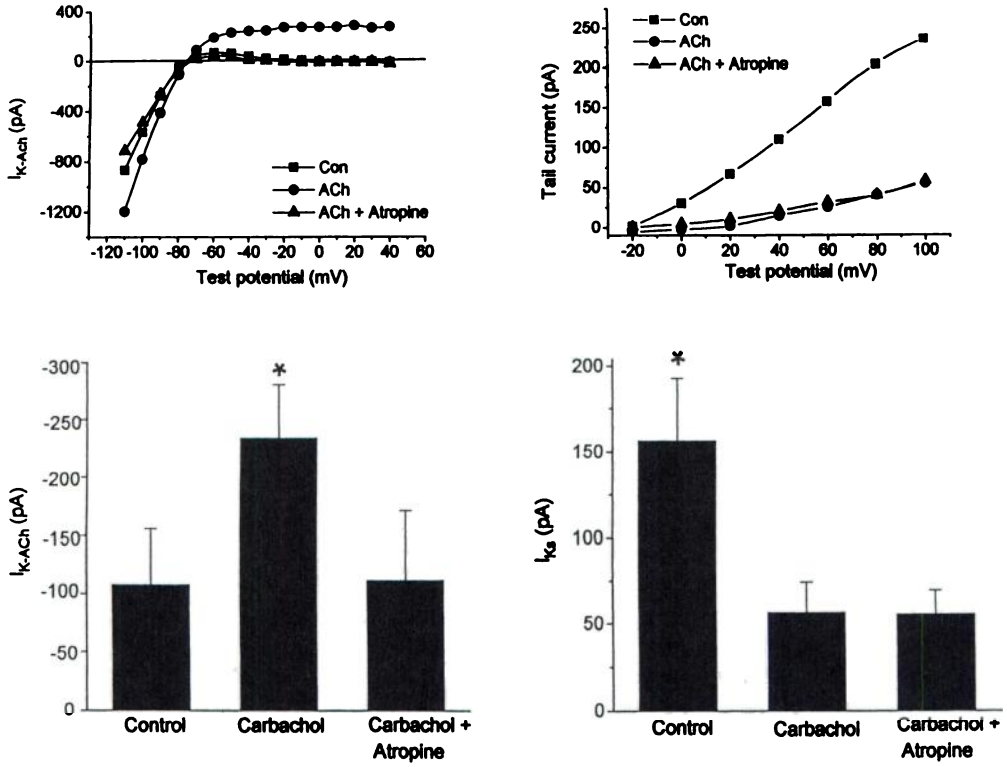

Fig. 4. Evidence that inhibition of I_{Ks} was not antagonized by atropine in cells where stimulation of $I_{K\text{-}ACh}$ was successfully reversed. *Right, upper*, enhancement of $I_{K\text{-}ACh}$ by extracellular application of 4 μM ACh in a cell isolated from the SAN region of guinea pig heart. Subsequent addition of 3 μM atropine antagonized stimulation of $I_{K\text{-}ACh}$. Current measured at the end of a 50-msec pulse was plotted against pulse potential (holding potential, −40 mV). Leak subtraction was used. Measurements were made in the whole-cell configuration, with an extracellular K^+ concentration of 5.0 mM, at 22°. *Con*, control. *Lower*, cumulative results from five experiments. $I_{K\text{-}ACh}$ was elicited in response to a 50-msec pulse to −90 mV, under control conditions and in the presence of carbachol (1 μM) or carbachol plus atropine (1 μM). Recording conditions were as described above. *Left, upper*, ACh inhibition of I_{Ks}, which was not reversed by atropine. Tail current amplitude associated with a 3-sec test pulse is plotted against pulse potential (same cell as shown in *right*). *Lower*, cumulative results from five experiments. I_{Ks} was measured as tail current amplitude after a 3-sec pulse to +60 mV from a −40-mV holding potential. Measurements were made in the whole-cell configuration, with an extracellular K^+ concentration of 5.0 mM, at 22°. *, Statistically significant differences in current amplitude.

on I_{Ks} and $I_{K\text{-}ACh}$ in cells previously treated with carbachol were similar to those of atropine (n = 2). Therefore, the failure of atropine to antagonize carbachol inhibition of guinea pig SAN I_{Ks} could not be attributed to either lack of muscarinic antagonist activity or absence of muscarinic receptors on isolated SAN cells under our experimental conditions.

Carbachol is an agonist that stimulates both muscarinic and nicotinic cholinoceptors. Nicotinic receptor stimulation has been reported to affect K^+ efflux in guinea pig SAN tissue preparations (20). To ascertain whether the atropine-insensitive inhibition of I_{Ks} by carbachol could be mediated by nicotinic receptors, we determined whether hexamethonium, a nicotinic receptor antagonist, could reverse carbachol inhibition of I_{Ks}. Neither hexamethonium alone nor the combination of hexamethonium and carbachol antagonized carbachol inhibition of SAN I_{Ks} (Fig. 5). Hexamethonium was without effect on carbachol inhibition of I_{Ks}, regardless of the order in which agonist and antagonist were applied (data not shown). When $I_{K\text{-}ACh}$ was measured in cells exposed sequentially to 1) hexamethonium, 2) hexamethonium and carbachol, and 3) hexamethonium, carbachol, and atropine, the muscarinic antagonist atropine but not the nicotinic antagonist hexamethonium reversed carbachol stimulation of $I_{K\text{-}ACh}$ (Fig. 5).

ACh and its stable analogue carbachol are structurally similar choline esters with quaternary ammonium groups. Quaternary ammonium compounds such as tetraethylammonium and tetramethylammonium are established as K^+ channel blockers and agonists of both muscarinic and nicotinic cholinoceptors (21, 22). To determine whether either a quaternary nitrogen moiety or an ester group is required for inhibition of I_{Ks}, we examined the effects of two additional muscarinic agonists. Oxotremorine [1-[4-(1-pyrrolidinyl)-2-butynyl]-2-pyrrolidinone] is a tertiary amine that is structurally dissimilar from other muscarinic agonists. OXA-22 is a potent pentatomic cyclic agonist that is structurally related to muscarine. Extracellular application of both compounds decreased the amplitude of guinea pig SAN I_{Ks} (Fig. 6). Atropine did not antagonize the effect of either oxotremorine (n = 3) or OXA-22 (n = 2). These data suggest that neither a quaternary nitrogen moiety nor an ester group is required for agonist inhibition of I_{Ks}.

Allosteric modulators of the muscarinic cholinoceptor can be tertiary as well as quaternary amines, and many allosteric antagonists also interact with K^+ channels (23, 24). Indeed, it is possible that the cholinergic agonists examined in this study inhibit I_{Ks} by interacting directly with the SAN slow delayed-rectifier K^+ channel. Verapamil is one of a number of drugs that have been shown both to modulate muscarinic receptors in an allosteric fashion (23, 24) and to block I_{Ks} (25, 26). We examined the effect of carbachol on I_{Ks} after inhib-

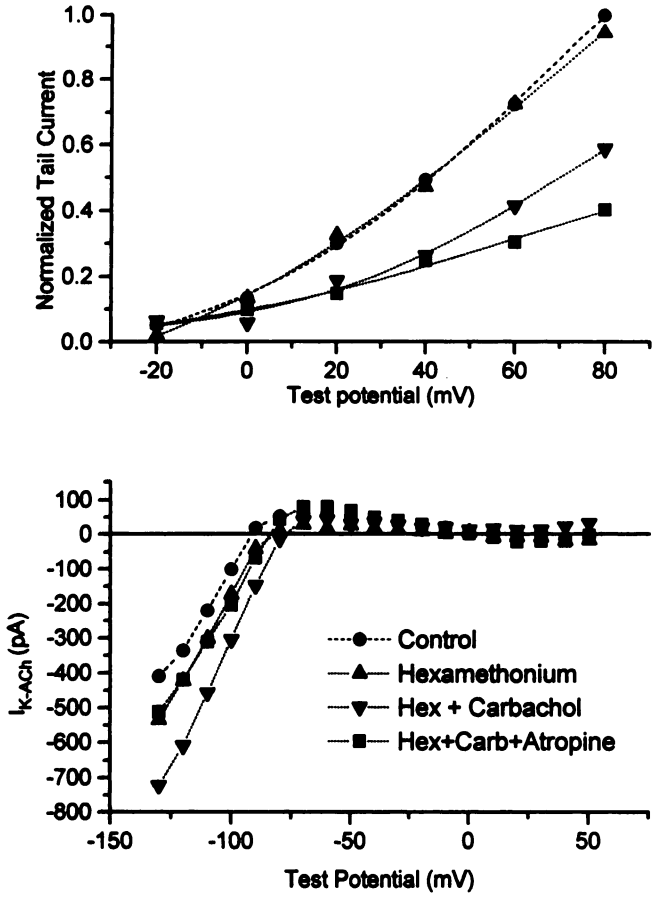

Fig. 5. Evidence that carbachol inhibition of I_{Ks} was not blocked by the nicotinic antagonist hexamethonium. *Upper*, normalized tail current plotted against test potential for I_{Ks}, measured as tail current amplitude after a 3-sec depolarizing test pulse from a holding potential of −40 mV under control conditions (●) and in the presence of hexamethonium (*Hex*) (▲), hexamethonium plus carbachol (*Carb*) (▼), or hexamethonium plus carbachol plus atropine (■). Measurements were made in the whole-cell configuration, with an extracellular K^+ concentration of 5.0 mM, at 22°. *Lower*, I_{K-ACh} measured at the end of 50-msec pulse plotted against pulse potential (holding potential, −40 mV) (same cell and experimental conditions as in *upper*).

iting the current with verapamil, and we found that the inhibitory effects of carbachol and verapamil were not additive (Fig. 7).

Discussion

The data presented demonstrate that cholinergic agonists, including the endogenous neurotransmitter ACh and its stable analogue carbachol, decrease the amplitude of I_{Ks} in guinea pig SAN cells via a non-muscarinic, non-nicotinic, cAMP-independent mechanism. Although the precise nature of this signal transduction pathway has not been elucidated, it is clearly different from those described previously for regulation of other nodal currents. Cholinergic regulation of I_{K-ACh}, I_{Ca}, and I_f in rabbit SAN is mediated by muscarinic receptors of the M2 subtype, whereas in guinea pig SAN stimulation of I_{K-ACh} but not inhibition of I_{Ks} by cholinergic agonists is mediated by muscarinic cholinoceptors (Figs. 4 and 5). Furthermore, in contrast to cholinergic inhibition of I_{Ca} and I_f in rabbit SAN, inhibition of I_{Ks} in guinea pig SAN is independent of intracellular cAMP concentration (Fig. 2).

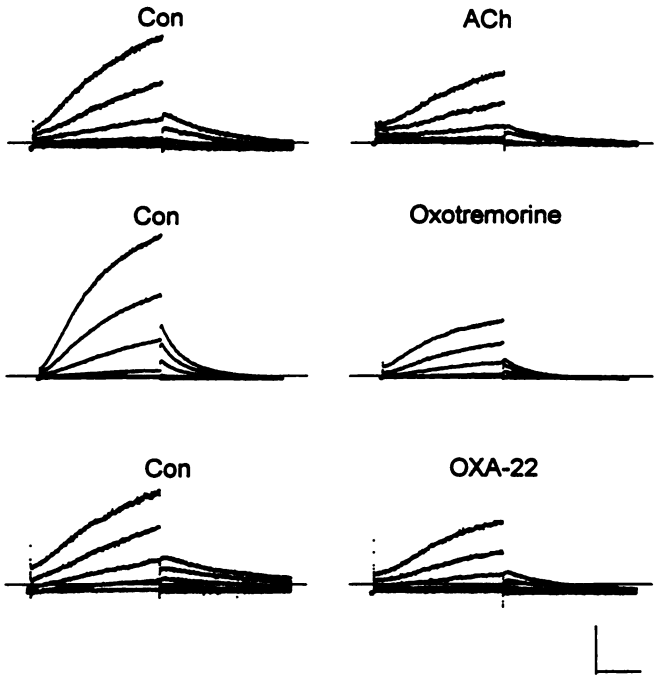

Fig. 6. Inhibition of I_{Ks} by three structurally dissimilar muscarinic agonists. *Left*, control (*Con*) currents; *right*, inhibition of I_{Ks} by ACh (500 nM) (*upper*) (*calibration bars*, 150 pA and 1000 msec), oxotremorine (500 nM) (*middle*) (*calibration bars*, 300 pA and 1500 msec), or OXA-22 (500 nM) (*lower*) (*calibration bars*, 100 pA and 1000 msec). Measurements were made in the whole-cell configuration, with an extracellular K^+ concentration of 0.5 mM, at 22°.

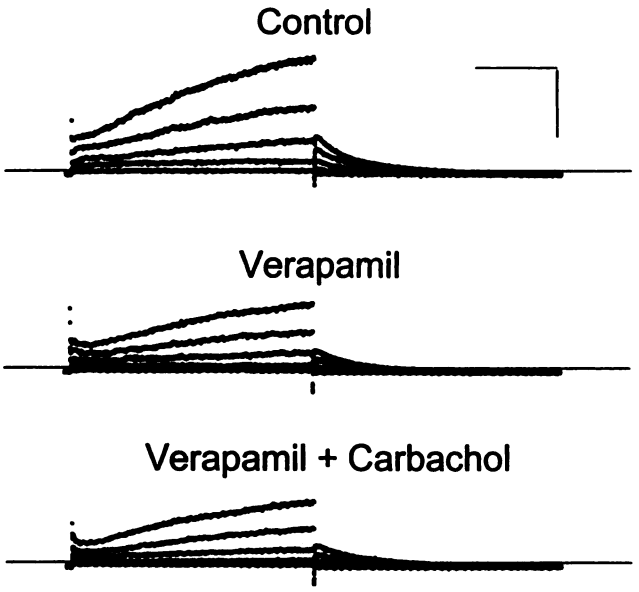

Fig. 7. Lack of additivity of inhibitory effects of verapamil and carbachol. I_{Ks} was recorded using a series of depolarizing test pulses (*bottom* to *top*, −20 to +60 mV, in steps of 20 mV) from a −40-mV holding potential, under control conditions and after extracellular application of verapamil (10 μM) and then verapamil plus carbachol (500 nM). *Calibration bars*, 50 pA and 1500 msec. Measurements were made in the whole-cell configuration, with an extracellular K^+ concentration of 0 mM, at 22°.

Differential regulation of I_{Ks} in guinea pig SAN and ventricle cannot be attributed to higher basal adenylate cyclase activity in SAN cells.

The data are consistent with the existence of either a novel

type of cholinoceptor in guinea pig SAN or a receptor-independent inhibitory interaction of cholinergic agonists with some distal component of the signal transduction pathway. Candidates for direct agonist interactions would include G proteins, regulatory enzymes, or the SAN delayed-rectifier K^+ channel itself. It is difficult to experimentally distinguish between these possibilities at the present time. The structure of the nodal slow delayed-rectifier K^+ channel is uncertain, and its regulation has not been completely characterized. Furthermore, there are no selective inhibitors of I_{Ks}. Receptor-independent interactions between cholinergic agonists and other components of a cytoplasmic signaling pathway cannot be ruled out as the cause of I_{Ks} inhibition in guinea pig SAN on the basis of the data presented. However, for the reasons detailed below, we favor a direct interaction between cholinergic agonists and the SAN channel protein as the basis for cholinergic inhibition of I_{Ks}.

It is generally assumed that the only cholinergic receptors found on isolated cardiocytes are muscarinic. Although the distribution of cholinergic receptors in guinea pig SAN has not been specifically examined, only muscarinic receptors of the M1 and M2 subtypes have been identified in guinea pig ventricle (27). To our knowledge, cholinoceptors sensitive to muscarinic agonists but insensitive to atropine have not been described in heart or any other tissue. It is improbable that such a unique population of receptors exists in guinea pig SAN.

Atropine-insensitive nicotinic cholinergic effects of ACh have been described by researchers studying isolated tissue preparations from the SAN region of guinea pig heart (20). However, our data preclude the possibility that inhibition of guinea pig SAN I_{Ks} is mediated by nicotinic receptor activation. Hexamethomium, at a concentration shown to selectively block nicotinic receptors (28), failed to antagonize the inhibition of I_{Ks} by carbachol (Fig. 5).

Direct interactions between cholinergic agonists and the SAN slow K^+ channel are quite plausible. There are many examples of drugs that interact with both muscarinic receptors and K^+ channels. For example, gallamine, methoctramine, verapamil, phencyclidine, and tetrahydroaminoacridine are known not only as allosteric antagonists of muscarinic receptors but also as blockers of K^+ currents, including I_{Ks} (23, 24). Likewise, quinidine, bretylium tosylate, and disopyramide are antiarrhythmic drugs that have been shown not only to block K^+ currents but also to interact with muscarinic receptors in an antagonistic fashion (29–33).

We determined the combined effects of the cholinergic agonist carbachol and the allosteric muscarinic antagonist verapamil on SAN I_{Ks} and found that the inhibitory effects of these two compounds are not additive (Fig. 7). Concentration-response curves for inhibition of I_{Ks} by both verapamil (25) and carbachol (Fig. 1) are extremely steep, with marked inhibition of I_{Ks} occurring over a narrow range of drug concentrations; furthermore, neither compound completely abolishes I_{Ks}. It is possible that these two compounds may inhibit I_{Ks} by a common mechanism.

A common structural feature of cholinergic agonists that block I_{Ks} and allosteric modulators of muscarinic receptors is that they are either quaternary amines or tertiary amines that would be protonated at physiological pH (23). Interactions of both agonists and allosteric antagonists with muscarinic cholinoceptors have been shown to depend on interactions between ligands and conserved aspartate residues in the receptor sequences, although different molecular entities are required for binding of agonists, compared with allosteric antagonists (34, 35). It is reasonable to speculate that negatively charged residues in the SAN I_{Ks} channel may be involved in inhibition of nodal I_{Ks} by cholinergic agonists. The biophysical characteristics and pharmacological profile of SAN I_{Ks} suggest that it is a minK channel (6, 17, 36). Aspartate residues just proximal to the transmembrane region of other cardiac minK channels have been shown to be important for inhibition of expressed minK currents by protons and La^{3+} (37–39). Furthermore, it has been hypothesized that alterations in surface charge play a role in inhibition of native cardiac delayed K^+ currents by cations and methoxyverapamil (26).

Minor sequence differences between species variants of minK channels have been linked to differences in kinetics and regulation of both expressed minK currents and the associated endogenous cardiac I_{Ks} (37, 40, 41). It is possible that small variations in amino acid sequence could also underlie regional differences in the regulation of I_{Ks}. Evaluation of this hypothesis will require cloning of the slow delayed-rectifier K^+ channel from guinea pig SAN.

References

1. Petit-Jacques, J., J. Bescond, P. Bois, and J. Lenfant. Particular sensitivity of the mammalian heart sinus node cells. *News Physiol. Sci.* **9**:77–79 (1994).
2. Chang, F., J. Gao, C. Tromba, I. Cohen, and D. DiFrancesco. Acetylcholine reverses effects of β-agonists on pacemaker current in canine cardiac Purkinje fibers but has no direct action: a difference between primary and secondary pacemakers. *Circ. Res.* **66**:633–636 (1990).
3. Harvey, R. D., and J. H. Hume. Autonomic regulation of delayed rectifier K^+ current in mammalian heart involves G proteins. *Am. J. Physiol.* **257**:H818–H823 (1989).
4. Yazawa, K., and M. Kameyama. Mechanism of receptor-mediated modulation of the delayed outward potassium current in guinea-pig ventricular myocytes. *J. Physiol. (Lond.)* **421**:135–150 (1990).
5. Petit-Jacques, J., P. Bois, J. Bescond, and J. Lenfant. Mechanism of muscarinic control of the high-threshold calcium current in rabbit sino-atrial node myocytes. *Pfluegers Arch.* **423**:21–27 (1993).
6. Freeman, L. C., and R. S. Kass. Delayed rectifier potassium channels in ventricle and sino-atrial node of guinea pig: molecular and regulatory properties. *Cardiovasc. Drugs Ther.* **7**:627–635 (1993).
7. DiFrancesco, D., and C. Tromba. Acetylcholine inhibits activation of the cardiac hyperpolarizing-activated current, I_f. *Pfluegers Arch.* **410**:139–142 (1987).
8. Yatani, A., and B. Brown. Regulation of cardiac pacemaker current I_f in excised membranes from sinoatrial node cells. *Am. J. Physiol.* **258**:H1947–H1951 (1990).
9. Irisawa, I., and N. Hagiwara. Ionic current in sinoatrial node cells. *J. Cardiovasc. Electrophysiol.* **2**:531–540 (1991).
10. Kotake, H., I. Hisatome, S. Matsuoka, H. Miyakoda, J. Hasegawa, and H. Mashiba. Inhibitory effect of 9-amino-1,2,3,4-tetrahydroacridine (THA) on the potassium current of rabbit sino-atrial node. *Cardiovasc. Res.* **24**: 42–46 (1990).
11. Walsh, K. B., and R. S. Kass. Regulation of a heart potassium channel by PKA and -C. *Science (Washington D. C.)* **242**:67–69 (1988).
12. Shibasaki, T. Conductance and kinetics of delayed rectifier potassium channels in nodal cells of the rabbit heart. *J. Physiol. (Lond.)* **387**:227–250 (1987).
13. Sanguinetti, M. C., and N. K. Jurkiewicz. Two components of cardiac delayed rectifier K^+ current. *J. Gen. Physiol.* **96**:195–215 (1990).
14. Carmeliet, E. Voltage- and time-dependent block of the delayed rectifier K^+ current in cardiac myocytes by dofetilide. *J. Pharmacol. Exp. Ther.* **262**: 809–817 (1992).
15. Sanguinetti, M. C., N. K. Jurkiewicz, A. Scott, and P. K. S. Siegl. Isoproterenol antagonizes prolongation of refractory period by the class III antiarrythmic agent E-4031 in guinea pig myocytes: mechanism of action. *Circ. Res.* **68**:77–84 (1991).
16. Freeman, L. C., and R. S. Kass. Carbachol inhibits delayed rectifier K^+ current in guinea pig sino-atrial node by a novel mechanism. *Circulation* **88**:1–34 (1993).
17. Anumonwo, J. M. B., L. C. Freeman, W. M. Kwok, and R. S. Kass. Delayed rectification in single cells isolated from guinea pig sino-atrial node. *Am. J. Physiol.* **262**:H921–H925 (1992).

18. Hamill, O. P., A. Marty, E. Neher, B. Sakmann, and F. J. Sigworth. Improved patch-clamp techniques for high resolution current recordings from cells and cell-free membrane patches. *Pfluegers Arch.* **391**:85–100 (1981).
19. Horn, R., and A. Marty. Muscarinic activation of ionic currents measured by a new whole-cell recording method. *J. Gen. Physiol.* **92**:145–159 (1988).
20. Lipsius, S. L., and M. Vasalle. Effects of acetylcholine on potassium movements in guinea pig sinus node. *J. Pharmacol. Exp. Ther.* **201**:669–677 (1977).
21. Kass, R. S., T. Scheuer, and K. J. Malloy. Block of outward current in cardiac Purkinje fibers by injection of quaternary ammonium ions. *J. Gen. Physiol.* **79**:1041–1063 (1982).
22. Zakharov, S. I., J. Overholt, R. A. Wagner, and R. D. Harvey. Tetramethylammonium activation of muscarinic receptors in cardiac ventricular myocytes. *Am. J. Physiol.* **264**:C1625–C1630 (1993).
23. Lee, N. H., and E. E. El-Fakahany. Allosteric antagonists of the muscarinic acetylcholine receptor. *Biochem. Pharmacol.* **42**:199–205 (1991).
24. Lee, N. H., and E. E. El-Fakahany. Allosteric interactions at the m1, m2 and m3 muscarinic receptor subtypes. *J. Pharmacol. Exp. Ther.* **256**:468–479 (1991).
25. Hume, J. R. Comparative interactions of organic Ca^{++} antagonists with myocardial Ca^{++} and K^+ channels. *J. Pharmacol. Exp. Ther.* **234**:134–140 (1985).
26. Kass, R. S., and R. W. Tsien. Multiple effects of calcium antagonists on plateau currents in cardiac Purkinje fibers. *J. Gen. Physiol.* **66**:169–192 (1975).
27. Gallo, M. P., G. Alloatti, C. Eva, A. Oberto, and R. C. Levi. M_1 muscarinic receptors increase calcium current and phosphoinositide turnover in guinea-pig ventricular cardiocytes. *J. Physiol. (Lond.)* **471**:41–60 (1993).
28. Eglen, R. M., A. D. Michel, C. M. Cornett, E. A. Kunysz, and R. L. Whiting. The interaction of hexamethonium with muscarinic receptor subtypes *in vitro*. *Br. J. Pharmacol.* **98**:499–506 (1989).
29. Cohen-Armon, M., Y. I. Henis, Y. Kloog, and M. Sokolovsky. Interactions of quinidine and lidocaine with rat brain and heart muscarinic receptors. *Biochem. Biophys. Res. Commun.* **127**:326–332 (1985).
30. Gillard, M., F. Brunner, M. Waelbroeck, M. Svoboda, and J. Christophe. Bretylium tosylate binds preferentially to muscarinic receptors labelled with [^{3}H]oxotremorine M (SH or "high affinity" receptors) in rat heart and brain cortex. *Eur. J. Pharmacol.* **160**:117–124 (1989).
31. Mirro, M. J., A. S. Manalan, J. C. Bailey, and A. M. Watanabe. Anticholinergic effects of disopyramide and quinidine on guinea pig myocardium: mediation by direct muscarinic receptor blockade. *Circ. Res.* **47**:855–865 (1980).
32. Nakajima, T., Y. Kurachi, H. Ito, R. Takikawa, and T. Sugimoto. Anticholinergic effects of quinidine, disopyramide and procainamide in isolated atrial mycoytes: mediation by different molecular mechanisms. *Circ. Res.* **64**:297–303 (1989).
33. Waelbrock, M., P. Robberecht, P. De Neef, and J. Christophe. Effects of verapamil on the binding properties of rat heart muscarinic receptors: evidence for an allosteric site. *Biochem. Biophys. Res. Commun.* **121**:340–345 (1984).
34. Fraser, C. M., C. D. Wang, D. A. Robinson, J. D. Gocayne, and J. C. Venter. Site-directed mutagenesis of m1 muscarinic acetylcholine receptors: conserved aspartic acids play important roles in receptor function. *Mol. Pharmacol.* **36**:840–847 (1989).
35. Lee, N. H., J. Hu, and E. E. El-Fakahany. Modulation by certain conserved aspartate residues of the allosteric interaction of gallamine at the m1 muscarinic receptor. *J. Pharmacol. Exp. Ther.* **262**:312–321 (1992).
36. Freeman, L. C., and R. S. Kass. Expression of a minimal K^+ channel protein in mammalian cells and immunolocalization in guinea pig heart. *Circ. Res.* **73**:968–973 (1993).
37. Hice, R. E., K. Folander, J. J. Salata, J. S. Smith, M. C. Sanguinetti, and R. Swanson. Species variants of the I_{sK} protein: differences in kinetics, voltage dependence, and La^{3+} block of the currents expressed in *Xenopus* oocytes. *Pfluegers Arch.* **426**:139–145 (1994).
38. Sanguinetti, M., and N. K. Jurkiewicz. Lanthanum blocks a specific component of I_K and screens membrane surface charge in cardiac cells. *Am. J. Physiol.* **259**:H1881–H1889 (1990).
39. Yamane, T., T. Furukawa, S. Horikawa, and M. Hiraoka. External pH regulates the slowly activating potassium current I_{sK} expressed in *Xenopus* oocytes. *FEBS Lett.* **319**:229–232 (1993).
40. Varnum, M. D., A. E. Busch, C. T. Bond, J. Maylie, and J. P. Adelman. The min K channel underlies the cardiac potassium current I_{Ks} and mediates species-specific responses to protein kinase C. *Proc. Natl. Acad. Sci. USA* **90**:11528–11532 (1993).
41. Zhang, Z. J., N. K. Jurkiewicz, K. Folander, E. Lazarides, J. J. Salata, and R. Swanson. K^+ currents expressed from the guinea pig cardiac I_{sK} protein are enhanced by activators of protein kinase C. *Proc. Natl. Acad. Sci. USA* **91**:1766–1770 (1994).

Send reprint requests to: Robert S. Kass, Department of Physiology, University of Rochester School of Medicine, 601 Elmwood Ave., Box 642, Rochester, NY 14642-8642.